53 GBaud Electro-Absorption Modulator Integrated Lasers for Intra-Data Center Networks

Masahiro HONDA*, Akira TAMURA, Kan TAKADA, Kenji SAKURAI, Hironori KANAMORI, and Kazuhiro YAMAJI

To cope with the rapid increase in data traffic, 400 Gbit/s optical transceivers have been introduced in data center optical communication systems, requiring high-performance electro-absorption modulator integrated lasers (EMLs). We have developed four EMLs with center wavelengths of 1271, 1291, 1311, and 1331 nm, which meet the specifications for 400 Gbit/s optical transceivers. This paper describes the design and typical characteristics of these new EMLs.

1. Introduction

As smartphones have come into wide use, SNS and video subscription services have grown, and teleworking has become popular due to COVID-19, the volume of data traffic has steadily increased. To be in line with this trend, data centers have increasingly moved toward the introduction of 400 Gbit/s optical transceivers to their optical networks. Various standards exist for 400 Gbit/s optical transceivers. For standards such as DR4*[1] and FR4*[2], the electro-absorption modulator integrated laser (EML) is used for PAM4*[3] operation at 53 GBaud modulation (transmission rate = 106 Gbit/s). To achieve 400 Gbit/s transmission, DR4 uses four EMLs with a center wavelength of 1311 nm, while FR4 uses one EML each with center wavelengths of 1271, 1291, 1311, and 1331 nm.

Sumitomo Electric Device Innovations, Inc. has developed and manufactured EMLs for 10 Gbit/s and 25 Gbit/s operations[1]-[3]. Drawing on these achievements, we have recently developed EMLs capable of 53 GBaud-PAM4 operation (hereinafter referred to as "53 GBaud-PAM4 EMLs") with center wavelengths of 1271, 1291, 1311, and 1331 nm.

2. Device Design

2-1 Target specifications

Table 1 lists target specifications, for which we referred to the 400GBASE-FR4 specification defined by IEEE 802.3cu. The 1271, 1291, 1311, and 1331 nm center wavelengths are termed Lane 0, 1, 2, and 3, respectively. The relative intensity noise (RIN) is an indicator of the laser noise level. The transmitter dispersion eye closure quaternary (TDECQ) is an indicator of the quality of PAM4 waveforms. By reducing the RIN and widening the 3 dB bandwidth, it is possible to reduce the value of TDECQ.

2-2 Device structure

Photo 1 shows the newly developed 53 GBaud-PAM4 EML. The left side of the photo is a distributed feedback laser oscillating in a single mode and the right side is a modulator. A direct current is supplied to the laser to emit

Table 1. Target Specifications

Parameter		Specification	Unit
Signaling rate		53.125 ± 100 ppm	GBaud
Modulation format		PAM4	-
Wavelength	Lane 0	1264.5 to 1277.5	nm
	Lane 1	1284.5 to 1297.5	
	Lane 2	1304.5 to 1317.5	
	Lane 3	1324.5 to 1337.5	
Average relative intensity noise		≤ -147	dB/Hz
3 dB bandwidth		≥ 35	GHz
TDECQ		≤ 3.4	dB
Optical modulation amplitude		≥ 5.5	dBm
Extinction ratio		≥ 3.5	dB
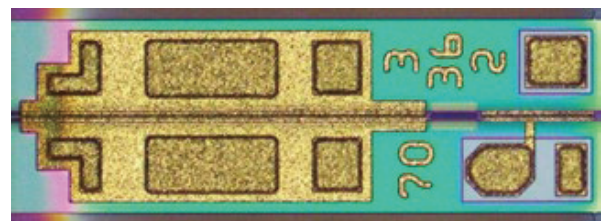
Photo 1. 53 GBaud-PAM4 EML

light at a certain intensity; a high-frequency electrical signal is applied to the modulator to produce a high-frequency optical signal.

Figure 1 presents a schematic cross section of the EML. Semiconductor layers were grown on an n-type indium phosphide (InP) substrate by metal organic chemical vapor deposition. Both the active layer of the laser and the absorption layer of the modulator comprise multiple quantum wells (MQWs). With these MQWs having different structures, both layers were connected by butt-joint growth technology. To reduce the reflection and scattering of light at the butt-joint, the optical intensity distri-
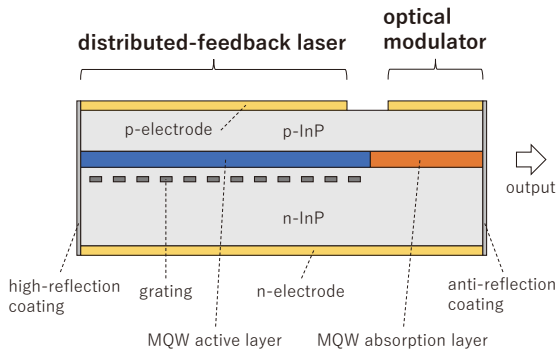
Fig. 1. Schematic cross section of EML

butions of the laser and modulator sections overlapped well. For the material of the facet coatings, highly moisture-resistant dielectrics were selected. Additionally, the front facet was coated with an anti-reflection coating to reduce the optical feedback to the laser, and the rear facet was coated with a high-reflection coating to improve optical output power.

2-3 Laser design

For the creation of a low-noise, high-power laser, it is necessary to optimize the laser MQWs. Figure 2 shows schematic band diagrams of laser MQWs. The well depth is important for both conduction and valence bands. First, for the conduction band, deeper wells are preferable. If the wells are shallow, electrons, being light, escape from shallow wells, degrading the characteristics [electron overflow, see Fig. 2 (a)]. In particular, care should be taken for Lane 0, which requires a larger band gap. Second, for the valence band, shallower wells are preferable. If the wells are deep, holes, being heavier than electrons, are injected only in the p-side wells, degrading the characteristics [non-uniform hole injection, see Fig. 2 (a)]. In this development, we optimized the structural parameters of laser MQWs to achieve deep conduction band wells and shallow valence band wells, as shown in Fig. 2 (b).
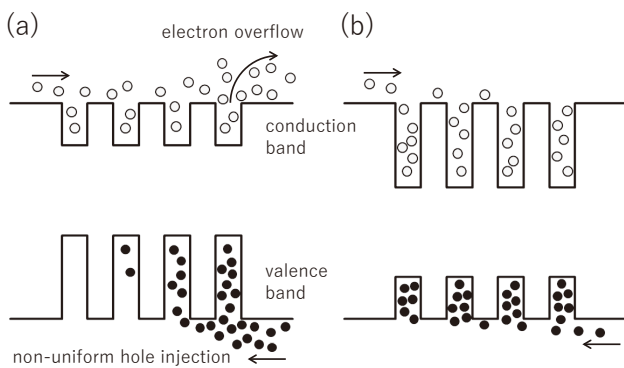
modulator quantum wells and wave functions observed when the voltage applied to the modulator (V_{MOD}) is 0 V (left) and when a reverse voltage is applied (right). The reverse voltage application reduces the band gap. This is known as the quantum-confined Stark effect (QCSE). Figure 3 (b) presents a schematic diagram of optical absorption spectra. When V_{MOD} is 0 V, modulator MQWs barely absorb laser light because the edge of the absorption spectrum is away from the lasing wavelength (λ_{LD}). On the other hand, reverse voltage application causes the edge of the absorption spectrum to shift toward the longer wavelengths due to the QCSE, allowing the modulator MQWs to absorb laser light, resulting in a lowered optical output power. In short, it is possible to control the optical output power by varying the voltage applied to the modulator.

To create a modulator with a high-bandwidth and a high-extinction ratio, important parameters are $\Delta\lambda$ [difference between the lasing wavelength and the edge of the absorption spectrum, see Fig. 3 (b)] and a modulator size. When the $\Delta\lambda$ is small, the laser light is mostly absorbed by the modulator and the optical output power becomes extremely low even if V_{MOD} is 0 V; when the $\Delta\lambda$ is large, the modulator absorbs the laser light minimally and the extinction ratio decreases because the edge of the absorption spectrum remains away from the lasing wavelength even under the application of a reverse voltage. In this development, the $\Delta\lambda$ was adjusted so that the extinction ratio would achieve the target. Next, regarding the modulator size, smaller ones are better in terms of bandwidth because the device capacitance decreases with decreasing the modulator size. However, for higher extinction ratios, it is necessary to raise the amount of light absorption by using a larger modulator size. In sum, a tradeoff exists between the bandwidth and the extinction ratio. In this development, we decided the modulator size by fully taking this tradeoff into account.
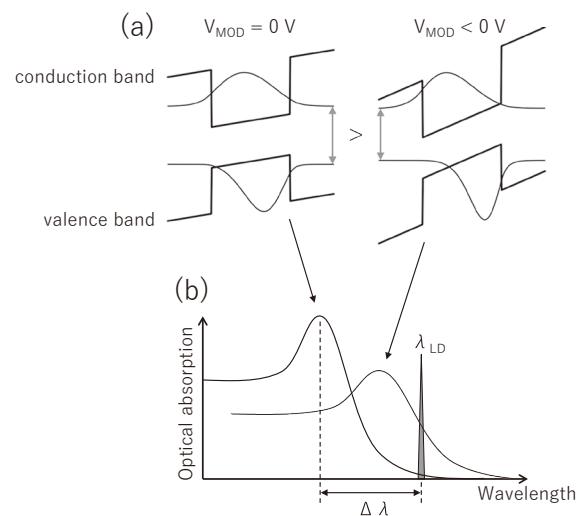
Fig. 3. Operating principle of modulator: (a) schematic diagrams of modulator quantum wells and wave functions and (b) optical absorption spectra

Fig. 2. Schematic band diagrams of laser MQWs

2-4 Modulator design

First, this section describes the operating principle of a modulator. Figure 3 (a) shows schematic diagrams of

3. Device Characteristics

3-1 Static characteristics

The optical and RIN spectra were evaluated as static characteristics. For these evaluations, the temperature was set to 60°C, the laser current was set to 100 mA, and the modulator voltage was set to 0 V.

Figure 4 shows the optical spectra. The bars indicate the target wavelength ranges listed in Table 1. In all lanes, the main peak is inside the indicated range, and the side mode suppression ratios (main peak to sub-peak ratios) are approximately 50 dB.
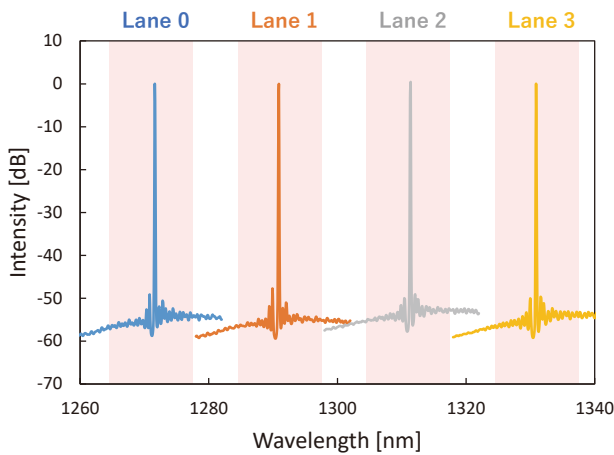
Fig. 4. Optical spectra

Figure 5 shows the RIN spectra. The average RIN values were –152.1, –152.0, –152.1, and –152.0 dB/Hz at Lane 0, 1, 2, and 3, achieving the target of –147 dB/Hz or less. Moreover, the maximum values observed around 10 GHz were –147 dB/Hz or less, with the device certainly demonstrating superb characteristics.
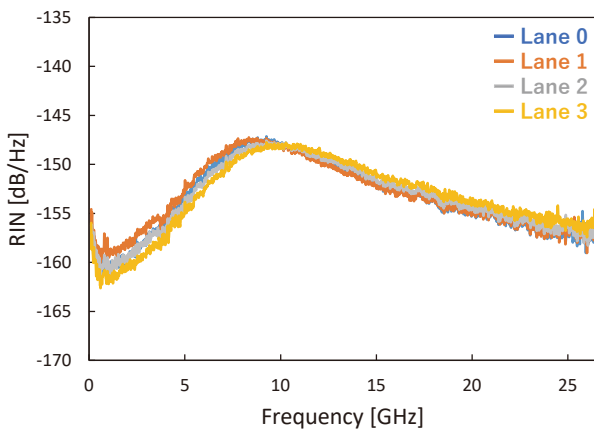
Fig. 5. RIN spectra

3-2 High-frequency characteristics

The frequency response and PAM4 optical waveforms were evaluated as high-frequency characteristics. For these evaluations, the temperature was set to 60°C and the laser current was set to 100 mA.

Figure 6 illustrates the experimental setup used to measure frequency response. The electrical signal output from the lightwave component analyzer traveled through the RF probe and entered the EML chip mounted on the submount. The optical signal emitted by the EML traveled through the optical fiber and entered the lightwave component analyzer. Figure 7 presents the measured frequency response. In all lanes, the 3 dB bandwidth reached approximately 41 GHz, well above the target of 35 GHz. The poor anti-reflection coating on the front facet is known to degrade frequency response flatness and to adversely affect the optical waveforms[4]. The newly developed EML has an almost flat frequency response up to approximately 30 GHz.
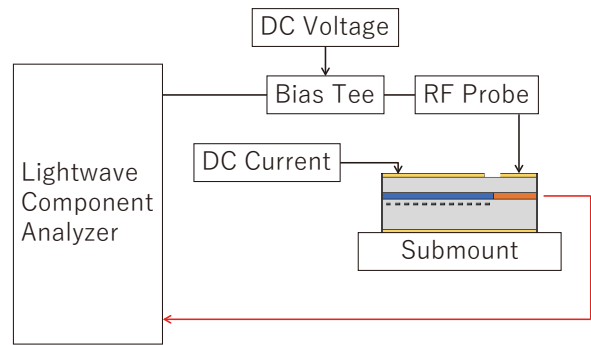
Fig. 6. Experimental setup for frequency response measurement
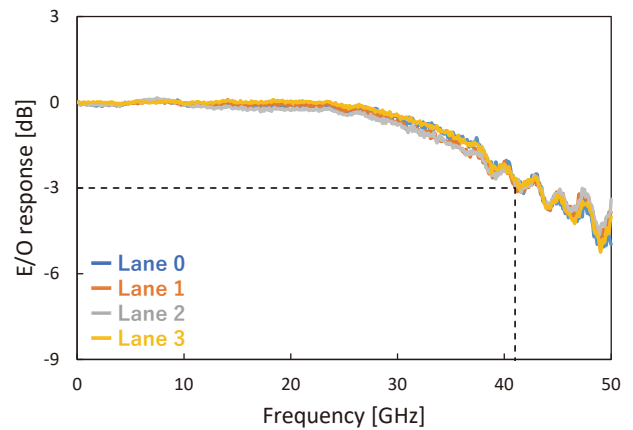
Fig. 7. Frequency responses

Figure 8 illustrates the experimental setup used to measure PAM4 optical waveforms. The arbitrary waveform generator generated a 53.125 GBaud-PAM4 electrical signal of the short stress pattern random quaternary (SSPRQ). Using an amplifier, the amplitude was adjusted to 1.2 V_{pp}. As performed for the frequency response evaluation, the electrical signal traveled through the RF probe

and entered the EML chip mounted on the submount. The optical signal emitted by the EML was captured by the oscilloscope and the signal was processed by an equalizer. Table 2 shows the measured PAM4 optical waveforms. In all lanes, clear eye openings were obtained and the TDECQ was favorable at 2 dB or less. Moreover, the extinction ratio was approximately 5 dB and the optical modulation amplitude was approximately 6.8 dB or more. Thus, we confirmed that our EMLs meet all the target specifications listed in Table 1.
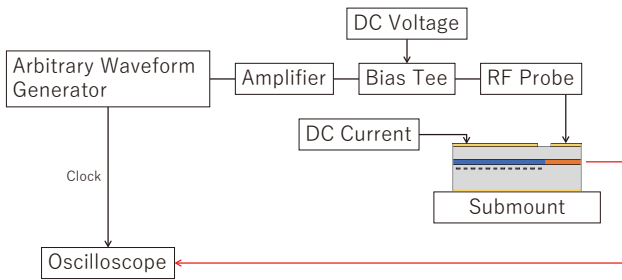
Fig. 8. Experimental setup for 53.125 GBaud PAM4 optical waveform measurement

4. Conclusion

We have developed 53 GBaud-PAM4 EMLs for 400 Gbit/s optical transceivers with center wavelengths of 1271, 1291, 1311, and 1331 nm. For low-noise and high-power operations, electron overflow and non-uniform hole injection were suppressed by optimizing laser MQWs. In addition, the $\Delta\lambda$ and modulator size were optimized to achieve both high bandwidth and high extinction ratio. The result was the average RIN of –147 dB/Hz or less and the 3 dB bandwidth of 35 GHz or more. In the optical waveform evaluation, the TDECQ was 2 dB or less, the extinction ratio was approximately 5 dB, and the optical modulation amplitude was approximately 6.8 dBm or more. The newly developed 53 GBaud-PAM4 EMLs for 400 Gbit/s optical transceivers have superb performance.

Technical Terms

∗1　DR4: The standardized specifications for optical transceivers with a transmission distance of up to 500 m.

∗2　FR4: The standardized specifications for optical transceivers with a transmission distance of up to 2 km.

∗3　PAM4: Four-level pulse amplitude modulation. The amount of information handled is double that of conventional two-level NRZ modulation.

References

(1)　H. Fukasawa et al., "Development of 10Gb/s TOSA/ROSA that Operates over Wide Temperature Range," SEI TECHNICAL REVIEW, No. 71 (October 2010)

(2)　H. Fujita et al., "25 Gbit/s Optical Transmitter Modules for Optical Transceiver," SEI TECHNICAL REVIEW, No. 80 (April 2015)

(3)　R. Teranishi et al., "Integrated TOSA with High-Speed EML Chips for up to 400 Gbit/s Communication," SEI TECHNICAL REVIEW, No. 86 (April 2018)

(4)　C. Sun et al., "Influence of Residual Facet Reflection on the Eye-Diagram Performance of High-Speed Electroabsorption Modulated Lasers," J. Lightw. Technol., vol. 27, no. 15, pp. 2970-2976 (August 2009)

Table 2. 53.125 GBaud-PAM4 optical waveforms

	Lane0	Lane1	Lane2	Lane3
Optical waveform (Back to Back)				
TDECQ [dB]	2.00	1.88	1.88	1.95
Extinction ratio [dB]	5.06	5.02	5.01	5.06
Optical modulation amplitude [dBm]	6.87	6.83	7.43	7.42

Contributors The lead author is indicated by an asterisk (∗).

M. HONDA∗
• Sumitomo Electric Device Innovations, Inc.

A. TAMURA
• Sumitomo Electric Device Innovations, Inc.

K. TAKADA
• Assistant General Manager, Sumitomo Electric Device Innovations, Inc.

K. SAKURAI
• Assistant General Manager, Sumitomo Electric Device Innovations, Inc.

H. KANAMORI
• Assistant General Manager, Sumitomo Electric Device Innovations, Inc.

K. YAMAJI
• Senior Assistant General Manager, Sumitomo Electric Device Innovations, Inc.